NeuroImage: Clinical 27 (2020) 102298

Contents lists available at ScienceDirect

NeuroImage: Clinical

journal homepage: www.elsevier.com/locate/ynicl

In vivo histopathological staging in *C9orf72*-associated ALS: A tract of interest DTI study

Hans-Peter Müller, Kelly Del Tredici, Dorothée Lulé, Kathrin Müller, Jochen H. Weishaupt, Albert C. Ludolph, Jan Kassubek*

Department of Neurology, University of Ulm, Germany

ARTICLE INFO

Keywords:
Diffusion tensor imaging
Amyotrophic lateral sclerosis
C9orf72 expansion
Magnetic resonance imaging
Motor neuron diseases

ABSTRACT

Background: Diffusion tensor imaging (DTI) can identify amyotrophic lateral sclerosis (ALS)-associated patterns of brain alterations at the group level according to a neuropathological staging system.
Objective: The study was designed to investigate the *in vivo* staging in ALS patients with the *C9orf72* expansion and potential differences to ALS patients with the *SOD1* mutation.
Methods: DTI-based white matter mapping was performed both by an unbiased voxel-wise statistical comparison and by a hypothesis-guided tract-wise analysis of fractional anisotropy (FA) maps according to the ALS-staging pattern for 27 ALS patients with *C9orf72* expansion vs 15 ALS patients with *SOD1* mutation vs 32 matched healthy controls. Clinical and neuropsychological data were acquired and correlated to DTI data.
Results: The analysis of white matter integrity demonstrated regional FA reductions along the CST and also in frontal and prefrontal brain areas according to the proposed propagation pattern for the ALS patients with *C9orf72* expansion and sporadic patients. This pattern could not be identified for the *SOD1* mutation at the group level. In contrast, in the tract-specific analysis according to the neuropathological ALS-staging pattern, *C9orf72* expansion ALS patients showed significant alterations of ALS-related tract systems similar to sporadic patients.
Conclusions: The DTI study including the tract-of-interest-based analysis showed a microstructural corticoefferent involvement pattern according to the staging scheme in *C9orf72*-associated ALS patients but not in the *SOD1* mutation.

1. Introduction

In 5–10% of patients with amyotrophic lateral sclerosis (ALS), a positive family history for ALS can be detected (familial ALS, fALS) (Chiò et al., 2011), and the research field of ALS continues to develop rapidly with multiple disease gene discoveries (Brenner and Weishaupt, 2019). An autosomal dominant inheritance of a GGGGCC hexanucleotide repeat in the first intron of the *C9orf72* gene is the most common cause of fALS in people of Northern European ancestry and is also a common cause of familial frontotemporal dementia (FTD) (Byrne et al., 2012; Renton et al., 2014; DeJesus-Hernandez et al., 2011; Rohrer et al., 2015). In the original publication describing that phosphorylated 43 kDa TAR DNA-binding protein (pTDP-43) pathology in ALS disseminates in a sequential pattern that permits recognition of four neuropathological stages (Brettschneider et al., 2013), the eleven cases with *C9orf72* repeat expansion displayed the same sequential spreading pattern as the nonexpansion cases despite a greater regional burden of lesions. The search for *in vivo* biomarkers of disease onset and progression in *C9orf72* repeat expansion carriers has yielded promising candidates, as summarized in a recent review (Floeter et al., 2018), with particular interest in neuroimaging as a biomarker because it offers – beyond the correlation of neuropathological data and *ex vivo* MRI (Pallebage-Gamarallage et al., 2018) – the option of visualizing pathological changes in the brains of living patients.

For the demonstration of cerebral TDP43 pathology according to the principles of the neuropathological staging concept of ALS (Brettschneider et al., 2013; Braak et al., 2013; Braak et al., 2017), a neuroimaging approach exists that uses a tract of interest (TOI)-based diffusion tensor imaging (DTI) analysis technique to demonstrate ALS-specific corticoefferent tract pathology *in vivo* (Kassubek et al., 2014; Kassubek et al., 2018). In the current study, a DTI- and TOI-based analysis was performed in patients with fALS and *C9orf72* expansion, comparing their findings with healthy controls and genetic ALS patients with *SOD1* mutation, to investigate the *in vivo* correlates of the neuropathological propagation pattern.

* Corresponding author at: Dept. of Neurology, University of Ulm, Oberer Eselsberg 45, 89081 Ulm, Germany.
E-mail address: jan.kassubek@uni-ulm.de (J. Kassubek).

https://doi.org/10.1016/j.nicl.2020.102298
Received 20 February 2020; Received in revised form 23 April 2020; Accepted 7 May 2020
Available online 26 May 2020

Table 1
(A) Patients' and controls' gender, age, and scanner distribution. (B) Subjects' characteristics including cognitive profile measured with the Edinburgh cognitive and behavioural ALS screen (ECAS) for statistical comparison.

(A)

	gender (m/f)	Age/years	age range/ years	MRI scanner 1.5 T/3.0 T
C9orf72	17/10	62 ± 12	34–78	22/5
controls A	23/9	59 ± 16	24–82	26/6
p (*t*-test)	0.47	0.49	–	0.98
SOD1	8/7	55 ± 13	37–79	12/3
controls B	12/9	54 ± 14	24–73	17/4
p (*t*-test)	0.69	0.90	–	0.94

(B)

	ECAS total score	memory	visuospatial	language	Verbal fluency	executive function	ALS-FRS-R median (range)	dis.dur./months median (range)	years of education	Handedness (right/left)	site of onset (spinal/ bulbar)
C9orf72	30 ± 8	13 ± 5	11 ± 2	22 ± 6	15 ± 5	30 ± 8	40 (34 – 48)	12 (3 – 37)	12.8 ± 3.8	26/1.	18/9
SOD1	107 ± 8	16 ± 2	12 ± 1	24 ± 4	17 ± 4.3	38 ± 4	44 (29 – 48)	13 (4 – 48)	13.7 ± 3.3	13/2.	15/0

2. Materials and methods

2.1. Subjects and patient characteristics

Forty-two patients with confirmed ALS mutations were included who clinically met the diagnostic criteria according to the El Escorial diagnostic criteria (Ludolph et al., 2015). The fALS patients included 27 *C9orf72* expansion carriers and a control group with a different mutation, i.e., 15 *SOD1* mutation carriers. Four of the *C9orf72* expansion carriers fulfilled the criteria for ALS-FTD of the behavioral type (bvFTD) according to Rascovsky criteria (Rascovsky et al., 2011). Details of demographics, clinical data including ALS-FRS-R (Cedarbaum et al., 1999), and disease duration for all groups are summarized in Table 1.

FALS patients were compared with a group of 32 age- and gender-matched controls. Gross brain pathology, including vascular brain alterations, could be excluded by conventional MRI including fluid attenuated inversion recovery sequences. All control individuals lacked a family history of neuromuscular disease and had no history of neurologic, psychiatric, or other major medical illnesses and were recruited from among spouses of patients and by word of mouth.

All participants provided written informed consent for the study protocol according to institutional guidelines which had been approved by the Ethics Committee of Ulm University, Germany (No. 19/12).

2.2. Cognitive analysis

In patients, cognition was measured with the German version (Lulé et al., 2015) of the Edinburgh Cognitive and Behavioral ALS Screen (ECAS) (Abrahams et al., 2014) by a trained psychologist. The ECAS addresses cognitive domains of language, verbal fluency, executive functions (ALS specific functions), and memory and visuospatial functions (ALS non-specific functions). Using the ECAS behavioral score, patients' behavioral alterations were reported by primary caregivers. Statistics for neuropsychology were performed using Statistical package for Social Sciences (SPSS version 21.0 IBM). Cognitive performance between groups was calculated with ANOVA and post-hoc Scheffé. Threshold of $p < 0.05$ was adopted for statistical significance.

2.3. Genetic analysis

DNA was extracted from whole EDTA-containing venous blood samples as previously described: analysis of the *C9orf72* repeat length was performed by fragment length analysis and repeat-primed PCR (RP-PCR) using previously published primers (Zondler et al., 2016). Since PCR-based methods cannot determine the size of larger expanded repeat-alleles, samples with a sawtooth pattern in the RP-PCR were further analyzed using Southern blot (DeJesus-Hernandez et al., 2011). *SOD1* genotyping was performed based on Sanger Sequencing using previously published primers (Waibel et al., 2010).

All *SOD1* mutations were missense mutations. The *SOD1*-patients had nine different mutations. The p.R116G mutation, the most frequent *SOD1* mutation in Germany, was represented four times, the p.H44R three times, and the p.V149A two times. Therefore we had a rather wide variety of *SOD1* mutations in our *SOD1* cohort. The number of repeats in the *C9orf72*-patients ranged from 750 to 3000. Given the heterogeneity in disease duration and rate of progression among different SOD1 mutations and the wide range of expansion lengths in our *C9orf72*-patients, we judge the results to be reliable independent of the type of *SOD1* mutations and the number of repeats in *C9orf72*.

The *SOD1*- as well as the *C9orf72*-associated ALS patients were from all over Germany. Two *C9orf72*-patients were from outside Germany, Austria and France, and one *SOD1*-patient was from Sweden. About 34% of the *C9orf72*-patients had a FTD co-morbidity, and one patient with a p.H49R mutation in *SOD1* presented symptoms that were consistent with a beginning bvFTD. The majority of the other family members with a *C9orf72* expansion had ALS alone, a subset of the index

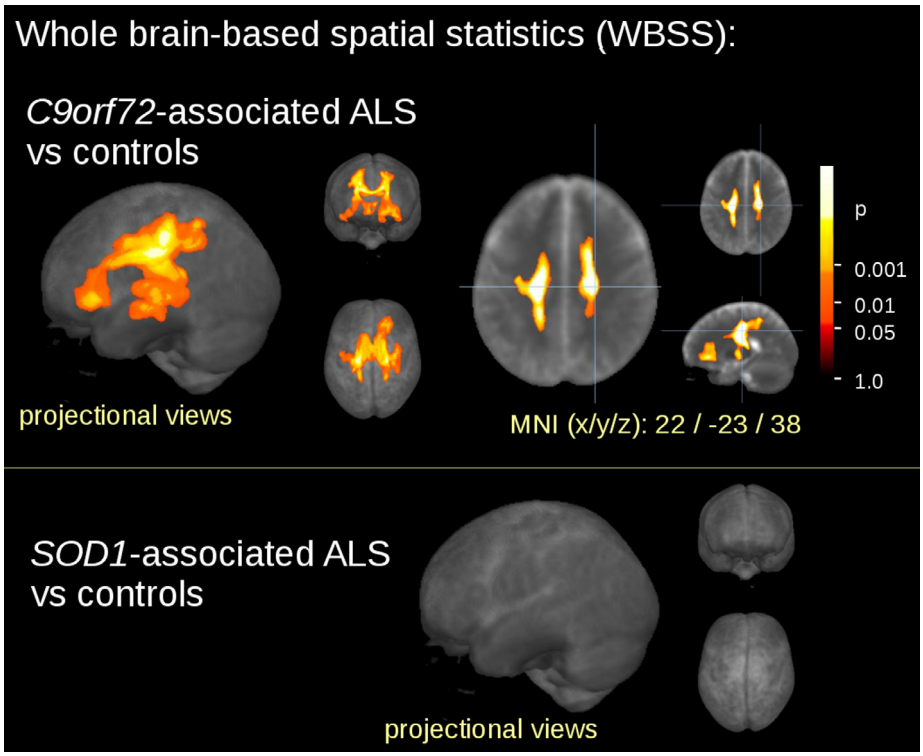

Fig. 1. Whole brain-based spatial statistics (WBSS) of FA maps of fALS patients vs controls. WBSS of FA maps ($p < 0.05$, False-discovery-rate (FDR) corrected) demonstrated one cluster of regional FA reductions for *C9orf72* fALS patients vs controls. The *SOD1* mutation did not show any significant cluster of FA reduction when compared to age- and gender-matched controls.

patients displayed cognitive or behavioural symptoms of FTD. ALS/FTD co-morbidity was rarely observed in those family members.

2.4. MRI acquisition

MRI scans were obtained with two scanners, a 1.5 Tesla Magnetom Symphony and a 3.0 T head scanner Allegra (both, Siemens Medical, Erlangen, Germany). The 1.5 T DTI study protocol consisted of 52 volumes (64 slices, 128x128 pixels, slice thickness 2.8 mm, pixel size 2.0 mm × 2.0 mm), representing 48 gradient directions (b = 1000 s/mm^2) and four scans with b = 0; TE and TR were 95 ms and 8000 ms. The 3.0 T DTI study protocol consisted of 49 volumes (52 slices, 96x128 pixels, slice thickness 2.2 mm, pixel size 2.2 mm × 2.2 mm), representing 48 gradient directions (b = 1000 s/mm^2) and one scan with b = 0; TE and TR were 85 ms and 7600 ms.

2.5. Data analysis

The analysis of the DTI data was performed by use of the software *Tensor Imaging and Fiber Tracking* (TIFT – Müller et al., 2007A). The algorithms used in this study have been previously described in detail (Kassubek et al., 2014; Kassubek et al., 2018; Müller and Kassubek, 2018). Stereotaxic normalization to the Montreal Neurological Institute (MNI) space was performed iteratively using study-specific templates (Müller et al., 2009). From the stereotaxically normalized DTI data sets of all subjects, fractional anisotropy (FA) maps were quantitatively calculated to map white matter microstructure (Le Bihan et al., 2001). A Gaussian filter of 8 mm full width at half maximum was applied for smoothing of FA maps for a good balance between sensitivity and specificity (Unrath et al., 2010). Finally, FA maps were corrected for the covariate age. Data were harmonized between the two scanners used (Müller et al., 2016) – the harmonization procedure has already been established at multicenter level cross-sectionally (Müller et al., 2013; Müller et al., 2016) and longitudinally (Kalra et al., 2020). In addition, the ratio of scans acquired at each scanner was almost the same between the subject groups, i.e., the age-matched controls' data sets were matched to the ALS groups for number of scans at the different scanners (for details see Table 1).

Statistical comparison by Student's *t*-test was performed voxel-wise for FA values to detect changes between the subject groups (whole brain-based spatial statistics, WBSS). Voxels with FA values below 0.2 were not considered for statistical comparison, since cortical grey matter shows FA values up to 0.2 (Kunimatsu et al., 2004). Statistical results were corrected for multiple comparisons using the false-discovery-rate (FDR) algorithm at $p < 0.05$ (Genovese et al., 2002). Further reduction of the alpha error was performed by a spatial correlation algorithm that eliminated isolated voxels or small isolated groups of voxels in the size range of the smoothing kernel leading to a threshold cluster size of 256 voxels (Kassubek et al., 2018).

Defined tract systems according to the ALS-staging system (Braak et al., 2013; Ludolph and Brettschneider, 2015) were identified with the tract-of interest (TOI) approach (Kassubek et al., 2014; Kassubek et al., 2018). TOIs for the four ALS stages were the corticospinal tract (CST, representative for stage 1), the corticorubral and corticopontine tracts (corresponding to stage 2), the corticostriatal pathway (stage 3), and the proximal perforant path (stage 4). As a reference path, a tract originating from the corpus callosum (CC) area V was used where no involvement in ALS-associated neurodegeneration could be anticipated. Tract-wise fractional anisotropy statistics (TFAS (Müller et al., 2007B; Müller et al., 2013)) was performed by statistically comparing the FA values in each tract system between two subject groups (Student's *t*-test), not considering FA-values < 0.2. The use of Student's *t*-test was justified since the groups were large enough to show a Gaussian distribution of FA values.

3. Results

3.1. Whole brain-based spatial statistics of FA maps

The WBSS comparison at the group level for the 27 *C9orf72* fALS patients vs 32 controls demonstrated widespread regional alterations (cluster size 63709 mm^3) at FDR-corrected $p < 0.05$ (Fig. 1): FA reductions were observed mainly along the CST (corresponding to neuropathological stage 1 of ALS – Kassubek et al., 2018) with projections

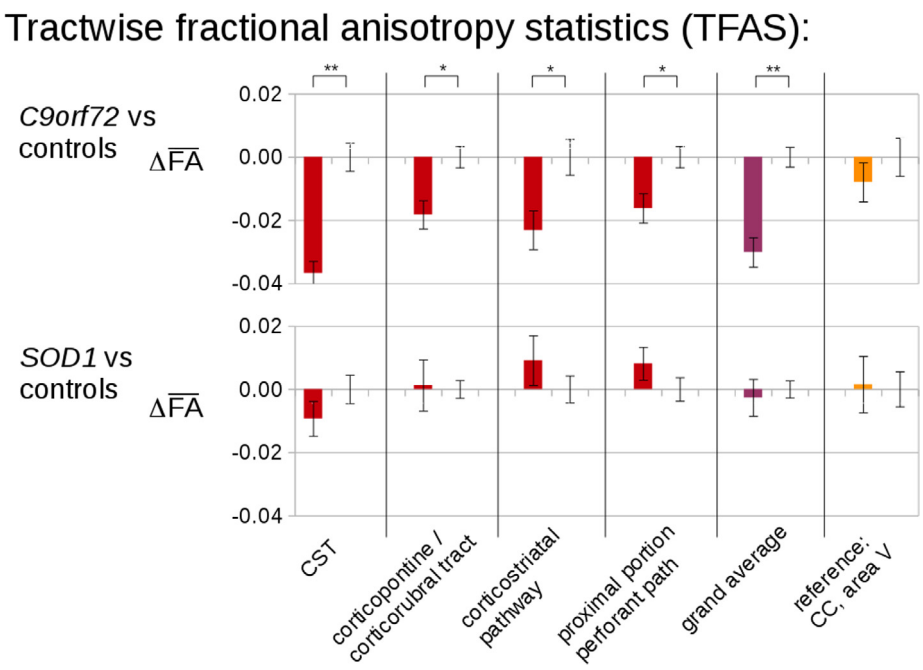

Fig. 2. Tractwise fractional anisotropy statistics (TFAS) of FA maps at the group level for fALS patients compared to controls. TFAS demonstrated significant regional FA reductions in ALS-related tract systems and in the grand average between *C9orf72* fALS patients and controls. *SOD1* mutation fALS patients did not show significant alterations when compared to age- and gender-matched controls. Error bars, SEM. * $p < 0.05$, ** $p < 0.001$.

to frontal areas (corresponding to neuropathological stages 2 and 3) and to the hippocampal areas (corresponding to neuropathological stage 4).

The comparison at the group level by WBSS for the 15 fALS patients with *SOD1* mutation vs 21 matched controls demonstrated no significant clusters of regional alterations at FDR-corrected $p < 0.05$.

3.2. Differences of FA in the specific tract systems

The analysis of the FA differences in the ALS-related tract systems by use of TFAS showed significant differences of the averaged FA values between the *C9orf27* fALS patients and control groups. Changes were most prominent in the CST, followed by FA reductions in the corticorubral and corticopontine tracts (i.e., tracts related to ALS stages 1 and 2) (Fig. 2). Further FA reductions could be observed for the corticostriatal pathway and for the proximal perforant path (i.e., the tracts related to ALS stages 3 and 4). For the grand average of the stage-related tract systems, significant FA reductions were observed accordingly. TFAS showed no significant differences of the averaged FA values between the *SOD1* fALS patients and controls (Fig. 2). No significant FA alterations were observed in the reference path for any group comparison.

3.3. ALS staging at the individual level

ALS staging categorization was performed for all ALS patients, and 89% of the *C9orf72* fALS patients could be staged (Supplementary Fig. 1). After division into bulbar onset and spinal onset, the stage distribution of the spinal and bulbar onset was similar to the distribution of the whole group so that no significant difference in terms of staging could be observed between spinal and bulbar onset. The percentage of stageable C9orf72 fALS was higher than in previous studies in sporadic ALS patients (Kassubek et al., 2018). In contrast, *SOD1*-associated fALS patients showed FA reductions along the CST compared to controls, but no significant changes of the other tract systems according to the staging scheme so that no staging categorization was possible in any of these fALS subjects. After division into bulbar onset and spinal onset, the stage distribution of the spinal and bulbar onset was similar to the distribution of the whole group so that no significant difference in terms of staging could be observed between spinal and bulbar onset.

3.4. Neuropsychology

C9orf72 patients performed worse in executive function (ANOVA $F = 4.09$, $p = 0.03$ with post-hoc Scheffé $p = 0.041$) and total score (trend ANOVA $F = 3.06$, $p = 0.06$ with post-hoc Scheffé $p = 0.069$) compared to *SOD1* patients. No differences between groups was observed for any of the other cognitive domains.

4. Discussion

This DTI study with a TOI-based analysis showed the same corticoefferent tract involvement pattern according to the neuropathological staging scheme in fALS patients with *C9orf72* expansion as previously reported for a large group of sporadic ALS patients (Kassubek et al., 2018), whereas this pattern could not be observed in ALS patients with *SOD1* mutation. On the basis of these neuroimaging data, the proposed staging scheme for ALS (Braak et al., 2013) could be confirmed *in vivo* for fALS with *C9orf72* expansion, in analogy with the demonstration of corticofugal tract involvement in 'classical' ALS (Kassubek et al., 2014; Kassubek et al., 2018) and in restricted ALS phenotypes (Rosenbohm et al., 2016; Müller et al., 2018A; Müller et al., 2018B; Müller et al., 2018C; Müller et al., 2019). Given that the neuropsychological results demonstrated that *C9orf72* patients performed significantly worse compared to *SOD1* patients, cognitive data underline the understanding that *C9orf72* ALS-patients resemble the subgroup within ALS that is closer to FTD according to neuropsychology than other genetic mutation carriers.

This is the first DTI study in patients with fALS with a hypothesis-guided TOI-based approach that addressed the white matter tracts corresponding to the pTDP-43-based neuropathology pattern. Previous data-driven DTI studies in fALS patients with *C9orf72* expansion in cross-sectional and longitudinal design demonstrated alterations in motor tracts, including the CST and the motor segment of the corpus callosum (Floeter et al., 2018; Agosta et al., 2017) and in the frontal white matter (Westeneng et al., 2016). In addition, further white matter areas and several white matter tracts were found to be affected: extensive cortico-striatal degeneration has been previously described in *C9orf72*-associated ALS, consistent with stage 3 (Omer et al., 2017).

Furthermore, extensive temporal lobe white matter alterations were also identified in *C9orf72* repeat carriers (Bede et al., 2018). The current hypothesis-based approach was able to define an involvement pattern that *per se* did not differ from sporadic ALS patients but was identical to that proposed by the neuropathological data (Brettschneider et al., 2013). In contrast to the *C9orf72* expansion-associated fALS, the *SOD1*-associated fALS patients showed no TOI-based abnormalities, probably due to a different pattern of neuropathology. The lack of significant cerebral alterations in the *SOD1* patients is in accordance with a previous study in 20 patients with *SOD1*-associated ALS who demonstrated a relative preservation of brain motor structural networks as assessed by DTI (Agosta et al., 2018).

This study was not without limitations. First, the neuropathological confirmation of the neuroimaging transfer of the ALS propagation scheme in the brain by autopsy results was not available for the patients studied. A second drawback was the limited number of available genotyped fALS patients, although it seems safe to conclude that the data from the original neuropathological study (Brettschneider et al., 2013) were sufficient to be generalized for all *C9orf72* expansion-associated fALS cases. In addition, DTI data from two different scanners had to be included. However, given that controls and patients were equally distributed over scanner types, the group comparisons can be regarded as matched for scanner type. Finally, future studies should include longitudinal data to investigate the possibility of tracking disease propagation, as previously demonstrated for sporadic ALS patients (Kassubek et al., 2018). Longitudinal tracking could optimally be performed in presymptomatic mutation carriers with respect to stagewise propagation, given that previous studies captured CST, CC and thalamic pathology long before projected symptom onset (Wen et al., 2019; Feis et al., 2019; Chen & Kantarci, 2020).

In summary, the tract-specific DTI analysis demonstrated alterations of ALS-related tract systems for *C9orf72*-associated fALS and, thus, might be a promising candidate biomarker for patients with *C9orf72* repeat expansion (Floeter and Gendron, 2018). Potentially, this approach will enable to detect effects of disease-modifying therapeutic interventions in the future, provided that the longitudinal TOI mapping reveals identical patterns as in sporadic ALS patients (Kassubek et al., 2018; Kassubek & Müller, 2020). Perhaps even more importantly, persons known to carry the *C9orf72* expansion could receive MRI and TOI-based analyses at presymptomatic clinical stages in order to determine the time point in the disease course when the *in vivo* detection of the neuropathological disease stages is possible.

5. Statement

All human studies have been approved by the appropriate ethics committee and have therefore been performed in accordance with the ethical standards laid down in the 1964 Declaration of Helsinki and its later amendments.

CRediT authorship contribution statement

Hans-Peter Müller: Conceptualization, Data curation, Formal analysis, Investigation, Methodology, Software,Visualization, Writing - original draft. **Kelly Del Tredici:** Validation, Writing - review & editing. **Dorothée Lulé:** Formal analysis (Neuropsychology), Writing - review & editing. **Kathrin Müller:** Formal analysis (Genetic data), Writing - review & editing. **Jochen H. Weishaupt:** Validation, Writing - review & editing. **Albert C. Ludolph:** Validation, Writing - review & editing. **Jan Kassubek:** Conceptualization, Investigation, Visualization, Data curation, Supervision, Writing - original draft.

Funding

This study was supported by the German Research Foundation (Deutsche Forschungsgemeinschaft, DFG Grant Number LU 336/15-1), the German Network for Motor Neuron Diseases (BMBF 01GM1103A), and Deutsches Zentrum für Neurodegenerative Erkrankungen (DZNE).

Declaration of Competing Interest

The authors declare that they have no known competing financial interests or personal relationships that could have appeared to influence the work reported in this paper.

Acknowledgements

Sonja Fuchs is thankfully acknowledged for her generous help in the acquisition of MRI data. The authors would like to thank the Ulm University Center for Translational Imaging MoMAN for its support.

Appendix A. Supplementary data

Supplementary data to this article can be found online at https://doi.org/10.1016/j.nicl.2020.102298.

References

Abrahams, S., Newton, J., Niven, E., et al., 2014. Screening for cognition and behaviour changes in ALS. Amyotroph Lateral Scler. Frontotemporal Degener. 15, 9–14.
Agosta, F., Ferraro, P.M., Riva, N., et al., 2017. Structural and functional brain signatures of C9orf72 in motor neuron disease. Neurobiol. Aging 57, 206–219.
Agosta, F., Spinelli, E.G., Marjanovic, I.V., et al., 2018. Unraveling ALS due to SOD1 mutation through the combination of brain and cervical cord MRI. Neurology 90, e707–e716.
Bede, P., Omer, T., Finegan, E., et al., 2018. Connectivity-based characterisation of subcortical grey matter pathology in frontotemporal dementia and ALS: a multimodal neuroimaging study. Brain Imaging Behav. 12, 1696–1707.
Braak, H., Brettschneider, J., Ludolph, A.C., et al., 2013. Amyotrophic lateral sclerosis – a model of corticofugal axonal spread. Nat. Rev. Neurol. 9, 708–714.
Braak, H., Neumann, M., Ludolph, A.C., Del Tredici, K., 2017. Does sporadic amyotrophic lateral sclerosis spread via axonal connectivities? Neurol. Int. Open. 1, E136–E141.
Brenner, D., Weishaupt, J.H., 2019. Update on amyotrophic lateral sclerosis genetics. Curr. Opin. Neurol. 32, 735–739.
Brettschneider, J., Del Tredici, K., Toledo, J.B., et al., 2013. Stages of pTDP-43 pathology in amyotrophic lateral sclerosis. Ann. Neurol. 74, 20–38.
Byrne, S., Elamin, M., Bede, P., et al., 2012. Cognitive and clinical characteristics of patients with amyotrophic lateral sclerosis carrying a C9orf72 repeat expansion: a population-based cohort study. Lancet Neurol. 11, 232–240.
Cedarbaum, J.M., Stambler, N., Malta, E., et al., 1999. The ALSFRS-R: a revised ALS functional rating scale that incorporates assessments of respiratory function. BDNF ALS Study Group (Phase III). J. Neurol. Sci. 169, 13–21.
Chen, Q., Kantarci, K., 2020. Imaging biomarkers for neurodegeneration in presymptomatic familial frontotemporal lobar degeneration. Front. Neurol. 11, 80.
Chiò, A., Calvo, A., Moglia, C., et al., 2011. Phenotypic heterogeneity of amyotrophic lateral sclerosis: a population based study. J. Neurol. Neurosurg. Psychiatry 82,740e746.
DeJesus-Hernandez, M., Mackenzie, I.R., Boeve, B.F., et al., 2011. ExpandedGGGGCC hexanucleotide repeat in noncoding region of C9orf72 causes chromosome 9p-linked FTD and ALS. Neuron 72, 245–256.
Feis, R.A., Bouts, M.J.R.J., Panman, J.L., et al., 2019. Single-subject classification of presymptomatic frontotemporal dementia mutation carriers using multimodal MRI. Neuroimage Clin. 22, 101718.
Floeter, M.K., Gendron, T.F., 2018. Biomarkers for amyotrophic lateral sclerosis and frontotemporal dementia associated with hexanucleotide expansion mutations in C9orf72. Front. Neurol. 9, 1063.
Floeter, M.K., Danielian, L.E., Braun, L.E., Wu, T., 2018. Longitudinal diffusion imaging across the C9orf72 clinical spectrum. J. Neurol. Neurosurg. Psychiatry 89, 53–60.
Genovese, C.R., Lazar, N.A., Nichols, T., 2002. Thresholding of statistical maps in functional neuroimaging using the false discovery rate. Neuroimage 15, 870–878.
Kalra, S., Müller, H.P., Ishaque, A., et al., 2020. A prospective harmonized multicentre DTI study of cerebral white matter degeneration in ALS. Neurology. in press.
Kassubek, J., Müller, H.P., 2020. Advanced neuroimaging approaches in amyotrophic lateral sclerosis: refining the clinical diagnosis. Expert Rev. Neurother. 20, 237–249.
Kassubek, J., Müller, H.P., Del Tredici, K., et al., 2014. Diffusion tensor imaging analysis of sequential spreading of disease in amyotrophic lateral sclerosis confirms patterns of TDP-43 pathology. Brain 137, 1733–1740.
Kassubek, J., Müller, H.P., Del Tredici, K., et al., 2018. Imaging the pathoanatomy of amyotrophic lateral sclerosis in vivo: targeting a propagation-based biological marker. J. Neurol. Neurosurg. Psychiatry 89, 374–381.
Kunimatsu, A., Aoki, S., Masutani, Y., et al., 2004. The optimal trackability threshold of fractional anisotropy for diffusion tensor tractography of the corticospinal tract. Magn. Reson. Med. Sci. 3, 11–17.
Le Bihan, D., Mangin, J.F., Poupon, C., et al., 2001. Diffusion tensor imaging: concepts and applications. J. Magn. Reson. Imaging 13, 534–546.

Ludolph, A., Drory, V., Hardiman, O., et al., 2015. A revision of the El Escorial criteria - 2015. Amyotroph Lateral Scler Frontotemporal Degener. 29, 1–2.
Ludolph, A.C., Brettschneider, J., 2015. TDP-43 in amyotrophic lateral sclerosis - is it a prion disease? Eur. J. Neurol. 22, 753–761.
Lulé, D., Burkhardt, C., Abdulla, S., et al., 2015. The Edinburgh Cognitive and Behavioural Amyotrophic Lateral Sclerosis Screen: a cross-sectional comparison of established screening tools in a German-Swiss population. Amyotroph Lateral Scler Frontotemporal Degener. 16, 16–23.
Müller, H.P., Unrath, A., Ludolph, A.C., et al., 2007A. Preservation of diffusion tensor properties during spatial normalisation by use of tensor imaging and fibre tracking on a normal brain database. Phys Med Biol. 52,N99-109.
Müller, H.P., Unrath, A., Sperfeld, A.D., et al. 2007B. Diffusion tensor imaging and tractwise fractional anisotropy statistics: quantitative analysis in white matter pathology. Biomed Eng Online. 6,42.
Müller, H.P., Unrath, A., Riecker, A., et al., 2009. Intersubject variability in the analysis of diffusion tensor images at the group level: fractional anisotropy mapping and fiber tracking techniques. Magn. Reson. Imag. 27, 324–334.
Müller, H.P., Grön, G., Sprengelmeyer, R., et al., 2013. Evaluating multicenter DTI data in Huntington's disease on site specific effects: an ex post facto approach. Neuroimage Clin. 2, 161–167.
Müller, H.P., Turner, M.R., Grosskreutz, J., et al., 2016. A large-scale multicentre cerebral diffusion tensor imaging study in amyotrophic lateral sclerosis. J. Neurol. Neurosurg. Psychiatry 87, 570–579.
Müller, H.P., Kassubek, J., 2018. MRI-Based mapping of cerebral propagation in amyotrophic lateral sclerosis. Front. Neurosci. 12, 655.
Müller, H.P., Agosta, F., Riva, N., et al., 2018a. Fast progressive lower motor neuron disease is an ALS variant: a two-centre tract of interest-based MRI data analysis. Neuroimage Clin. 17, 145–152.
Müller, H.P., Gorges, M., Kassubek, R., et al., 2018b. Identical patterns of cortico-efferent tract involvement in primary lateral sclerosis and amyotrophic lateral sclerosis: a tract of interest-based MRI study. Neuroimage Clin. 18, 762–769.
Müller, H.P., Agosta, F., Gorges, M., et al., 2018c. Cortico-efferent tract involvement in primary lateral sclerosis and amyotrophic lateral sclerosis: A two-centre tract of interest-based DTI analysis. Neuroimage Clin. 20, 1062–1069.
Müller, H.P., Gorges, M., Del Tredici, K., et al., 2019. The same cortico-efferent tract involvement in progressive palsy and in 'classical' ALS: a tract of interest-based MRI study. Neuroimage Clin. 24, 101979.
Omer, T., Finegan, E., Hutchinson, S., et al., 2017. Neuroimaging patterns along the ALS-FTD spectrum: a multiparametric imaging study. Amyotroph. Lateral Scler. Frontotemporal. Degener. 18, 611–623.
Pallebage-Gamarallage, M., Foxley, S., Menke, R.A.L., 2018. Dissecting the pathobiology of altered MRI signal in amyotrophic lateral sclerosis: a post mortem whole brain sampling strategy for the integration of ultra-high-field MRI and quantitative neuropathology. BMC Neurosci. 19, 11.
Rascovsky, K., Hodges, J.R., Knopman, D., et al., 2011. Sensitivity of revised diagnostic criteria for the behavioural variant of frontotemporal dementia. Brain 134, 2456–2477.
Renton, A.E., Chiò, A., Traynor, B.J., 2014. State of play in amyotrophic lateral sclerosis genetics. Nat. Neurosci. 17, 17–23.
Rohrer, J.D., Isaacs, A.M., Mizielinska, S., et al., 2015. C9orf72 expansions in frontotemporal dementia and amyotrophic lateral sclerosis. Lancet Neurol. 14, 291–301.
Rosenbohm, A., Müller, H.P., Hübers, A., et al., 2016. Corticoefferent pathways in pure lower motor neuron disease: a diffusion tensor imaging study. J. Neurol. 263, 2430–2437.
Unrath, A., Müller, H.P., Riecker, A., et al., 2010. Whole brain-based analysis of regional white matter tract alterations in rare motor neuron diseases by diffusion tensor imaging. Hum. Brain Mapp. 31, 1727–1740.
Waibel, S., Neumann, M., Rabe, M., et al., 2010. Novel missense and truncating mutations in FUS/TLS in familial ALS. Neurology 75, 815–817.
Westeneng, H.J., Walhout, R., Straathof, M., et al., 2016. Widespread structural brain involvement in ALS is not limited to the C9orf72 repeat expansion. J. Neurol. Neurosurg. Psychiatry 87, 1354–1360.
Wen, J., Zhang, H., Alexander, D.C., et al., 2019. Neurite density is reduced in the presymptomatic phase of C9orf72 disease. J. Neurol. Neurosurg. Psychiatry 90, 387–394.
Zondler, L., Müller, K., Khalaji, S., et al., 2016. Peripheral monocytes are functionally altered and invade the CNS in ALS patients. Acta Neuropathol. 132, 391–411.